IOSUD - Politehnica University of Timisoara
Doctoral School of Engineering Studies

STRUCTURED MATERIALS WITH DESIGNED FUNCTIONALITY FOR Au(III) AND Pd(II) RECOVERY

PhD thesis – Abstract
for obtaining the scientific title of doctor engineer at
Politehnica University of Timisoara
in the PhD field of Chemical Engineering

Scientific coordinator,
Professor, PhD eng. Adina-Georgeta NEGREA

Author,
eng. IOSIF Maria (MIHĂILESCU)

April, 2022

CONTAINED

INTRODUCTION

As a result of the rapid progress of technology, obtaining of new materials with designed properties for the recovery of precious metals has become an important target of science. The strategies for obtaining these materials have undergone changes in line with the new economic and environmental requirements.

Many modern methods of recovery of precious metals have been developed, some of them have already been implemented on an industrial scale. The recovery of precious metals by adsorption on a variety of solid substrates has consistently gained increased attention in recent years. Particular attention has been paid to studies on the characterization of adsorption properties of materials with affinity for gold and palladium depending on the nature of the active groups present in the material structure.

The main objective of the research was to obtain new materials with functionality designed so to obtain materials with selective adsorption properties. Thus, new adsorbent materials were obtained by functionalizing by impregnation some inert solid supports, with extractants whose active groups are with nitrogen, carboxyl and sulfur. The target was the recovery by adsorption of gold and palladium from used solutions generated from industrial processes.

The studies in this doctoral thesis took into account a series of materials with high/selective adsorbent properties for the recovery of Au(III) and Pd(II) from the used solutions. Thus, 80 materials were synthesized by impregnation functionalization, using the ultrasonication method and the dry method - SIR (Solvent Impregnated Resin), of a solid support of inorganic nature – $MgSiO_3$, of two solid supports of organic nature from the class of commercial polymers - polymer resin of type Amberilte XAD7 (acrylic matrix) and resin of Amberlite XAD4 type (styrene matrix- divinylbenzene) and of a biopolymer - cellulose. The amino acids L-cysteine ($C_3H_7NO_2S$) and L-glutamic acid ($C_5H_9NO_4$) were used as a source of functional groups (extractants).

The new materials obtained by functionalization were characterized by physic-chemical methods. The adsorption properties of the new materials for the recovery of Au(III) and Pd(II) were highlighted. For this, adsorption studies have been performed in static and dynamic regime. The parameters influencing the adsorption process, respectively the adsorption capacity, have been studied, namely:

(i) for static adsorption, the following have been studied: the ratio solid: liquid, pH of the solutions, contact time, temperature and initial concentration of metal ions in the waste solution;

(ii) for dynamic adsorption, the following have been studied: the height of the material layer in the fixed bed adsorption column, the contact time in the adsorption column, the flow rate of the solutions containing the ions of precious metals.

In order to establish the mechanism of the adsorption process, kinetic studies, thermodynamics and equilibrium studies have been carried out.

In addition, in order to highlight the feasibility of the obtained materials, adsorption-desorption studies were carried out and the number of adsorption-desorption cycles was established.

The proposal for the recovery process of gold and palladium ions in metallic form from the exhausted adsorbent material is another target of this study.

In order to design adsorption processes on an industrial scale, the experimental data were optimized by factorial experiment; the objective function (in this case, the adsorption capacity) defines and quantitatively evaluates the behavior and trends of evolution of the adsorption process under investigation, starting from several controllable factors (pH, contact time, temperature, initial concentration of the metal ion in solution).

The structure of the thesis consists of 2 parts and 9 chapters, includes 42 tables and 100 figures, accompanied by 357 bibliographic references.

Part I refers to the study of literature and includes 4 chapters.

Part II contains the original contributions, the final conclusions, the bibliographical references and is structured throughout chapters 5 to 9.

CHAPTER 5. OBTAINING AND PHYSICOCHEMICAL CHARACTERIZATION OF THE MATERIALS OBTAINED BY FUNCTIONALIZATION BY IMPREGNATION

In order to improve the adsorbent properties of materials, in particular their adsorption capacity, adsorption being a common method of recovering metal ions from used solutions, the functionalization by impregnation of inert supports of organic or inorganic nature with active groups of N, P, S or -COOH is increasingly used.

Obtaining materials through functionalization

The materials studied for the adsorption recovery of Au(III) and Pd(II) were obtained by impregnation functionalization using the SIR (Solvent impregnated resin) method [292], but also by ultrasonication [293]. The method of obtaining the new materials was selected according to the adsorption capacity, selectivity, physico-chemical resistance in the aqueous environment, economic efficiency and the possibility of regeneration.

80 materials were synthesized, as follows:

- as a support were used: two commercial resins of the type Amberlite XAD4 (styrene-divinylbenzene matrix) and Amberlite XAD7 (acrylic matrix), an inorganic support - magnesium silicate, $MgSiO_3$ and a biopolymer - cellulose (C);
- amino acids were used as extractants: L-glutamic acid (AcLG) and L-cysteine (LCys);
- the support per mass ratio was varied: extractant, namely 1 g of support: (0,05; 0,10; 0,15; 0,20 and 0,30) g extractant.
- the synthesized materials were dried at 323 K for 24 h.

The following have been obtained:

Table 5.1

Adsorbtion capacity, q [mg/g]									
No.	Mass ratio support : AcLG	Support							
		Amberlite XAD4		Amberlite XAD7		$MgSiO_3$		Cellulose	
		Au(III)	Pd(II)	Au(III)	Pd(II)	Au(III)	Pd(II)	Au(III)	Pd(II)
1.	1 : 0.05	1.93	0.98	2.49	0.21	0.83	0.27	0.94	0.23
2.	1 : 0.10	2.35	1.02	2.50	0.22	0.83	0.31	1.06	0.45
3.	1 : 0.15	2,36	1.03	2.50	0.23	0.85	0.32	1.07	0.45
4.	1 : 0.20	2.38	1.23	2.50	0.24	0.87	0.33	1.07	0.47
5.	1 : 0.30	2.39	1.24	2.52	0.24	0.68	0.34	0.87	0.47

Adsorption capacity of materials which are obtained by functionalisation by the SIR method (Table 5.1, Table 5.2)

Table 5.2

Adsorbtion capacity, q [mg/g]									
No.	Mass ratio support : LCys	Support							
		Amberlite XAD4		Amberlite XAD7		$MgSiO_3$		Cellulose	
		Au(III)	Pd(II)	Au(III)	Pd(II)	Au(III)	Pd(II)	Au(III)	Pd(II)
1.	1 : 0.05	1.97	1.23	1.30	0.35	1.64	2.27	1.44	0.05
2.	1 : 0.10	2.08	1.22	1.37	0.49	1.72	2.33	1.43	1.50
3.	1 : 0.15	2.08	1.23	1.37	0.52	1.72	2.34	1.45	1.50
4.	1 : 0.20	2.08	1.22	1.38	0.52	1.71	2.34	1.46	1.51
5.	1 : 0.30	2.08	1.22	1.38	0.52	1.71	2.34	1.46	1.51

Table 5.3

Adsorbtion capacity, q [mg/g]									
No.	Mass ratio support : AcLG	Support							
		Amberlite XAD4		Amberlite XAD7		$MgSiO_3$		Cellulose	
		Au(III)	Pd(II)	Au(III)	Pd(II)	Au(III)	Pd(II)	Au(III)	Pd(II)
1.	1 : 0.05	1.96	1.04	2.51	0.25	0.99	0.30	1.75	0.95
2.	1 : 0.10	1.99	1.20	2.53	0.32	1.23	0.32	1.88	0.98
3.	1 : 0.15	2.01	1.21	2.54	0.33	1.24	0.33	2.30	0.98
4.	1 : 0.20	2.01	1.22	2.54	0.33	1.25	0.33	2.34	0.97
5.	1 : 0.30	2.01	1.22	2.54	0.33	1.25	0.33	2.48	0.76

Adsorption capacity of materials which are obtained by ultarsonation functionalization (Table 5.3, Table 5.4)

Table 5.4

Adsorbtion capacity, q [mg/g]									
No.	Mass ratio support : LCys	Support							
		Amberlite XAD4		Amberlite XAD7		$MgSiO_3$		Cellulose	
		Au(III)	Pd(II)	Au(III)	Pd(II)	Au(III)	Pd(II)	Au(III)	Pd(II)
1.	1 : 0.05	1.99	1.81	2.15	1.00	1.65	2.33	2.13	1.00
2.	1 : 0.10	2.18	1.85	2.32	1.16	1.72	2.38	2.28	1.58
3.	1 : 0.15	2.18	1.86	2.31	1.16	1.72	2.38	2.34	1.58
4.	1 : 0.20	2.18	1.86	2.33	1.16	1.72	2.38	2.33	1.58
5.	1 : 0.30	2.03	1.86	2.00	1.06	1.72	2.38	2.33	1.58

Thus, the support mass ratio: the optimal extractant to obtain the highest adsorption capacity was the support ratio : extractant = 1 : 0.1 g/g. Ultrasonication is a faster process (the

functionalization time by impregnation is 10 min) compared to the SIR method (the functionalization time by impregnation is 24h) so that the subsequent synthesises were achieved by functionalization by ultrasonication.

Physico-chemical characterization of materials obtained by functionalization by impregnation

The materials which are obtained by functionalization, selected for subsequent studies, were characterized by different physicochemical methods, namely: (i) scanning electron microscopy, SEM, (ii) X-ray spectroscopy with energy dispersion, EDX, (iii) infrared spectroscopy with fourier transform, FT-IR and (iv) atomic force microscopy, AFM. It was determined the specific area and the volume of pores by bet method (Brunauer-Emmet-Teller). At the same time, the zero load point, pH_{pZc} [297], was established.

Morphological and structural analysis by scanning electron microscopy, SEM and energy dispersion X-ray spectroscopy, EDX:

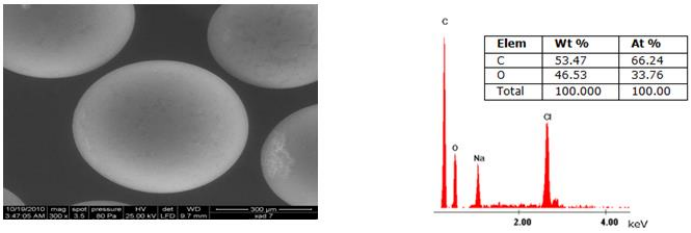

Elem	Wt %	At %
C	53.47	66.24
O	46.53	33.76
Total	100.000	100.00

(a) SEM image and EDX spectrum for Amberlite XAD7 solid support

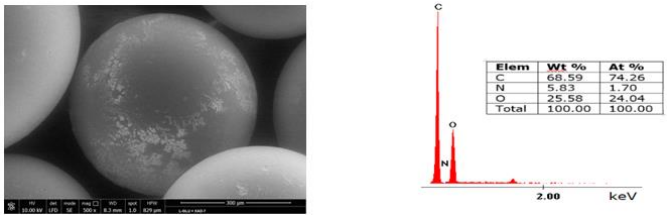

Elem	Wt %	At %
C	68.59	74.26
N	5.83	1.70
O	25.58	24.04
Total	100.00	100.00

(b) SEM image and EDX spectrum for XAD7-AcLG material

Figure 5.2. Scanning electron microscopy, SEM [337] and energy dispersion X-ray spectroscopy, EDX for XAD7 solid support (a) and XAD7-AcLG material (b) [297]

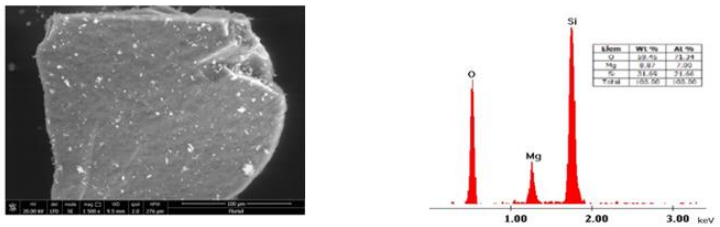

(a) SEM image and EDX spectrum for $MgSiO_3$ solid support

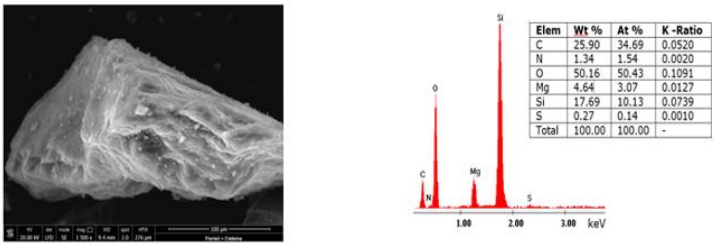

Elem	Wt %	At %	K-Ratio
C	25.90	34.69	0.0520
N	1.34	1.54	0.0020
O	50.16	50.43	0.1091
Mg	4.64	3.07	0.0127
Si	17.69	10.13	0.0739
S	0.27	0.14	0.0010
Total	100.00	100.00	-

b) SEM image and EDX spectrum for $MgSiO_3$-LCys material

Figure 5.3. Scanning electron microscopy, SEM and energy dispersion X-ray spectroscopy, EDX for MgSiO3 support (a) and $MgSiO_3$-LCys material (b) [303]

After the functionalization by impregnation, it was noticed that on the surface of the resin particles of type Amberlite XAD7 there were morphological changes specific to the presence of L-glutamic acid, and from the semi-quantitative analysis (EDX) of the XAD7-AcLG material it was observed the presence of a quantity of nitrogen (5,83%) specific to the -NH_2 group, which confirms the functionalization of the polymeric support with L-glutamic acid (Figure 5.3.a) [297].

In the case of $MgSiO_3$-LCys material, the SEM image shows small morphological changes after functionalization (Figure 5.3.b), changes that can be attributed to the presence of the amino acid L-cysteine.

At the same time, the EDX spectra confirm the presence of specific extractant picks: S, N, C from the functional groups –SH, -NH_2 and –COOH and specific to the support used: Si, O and Mg ($MgSiO_3$) [303].

Infrared spectroscopy with Fourier transform, FT-IR:

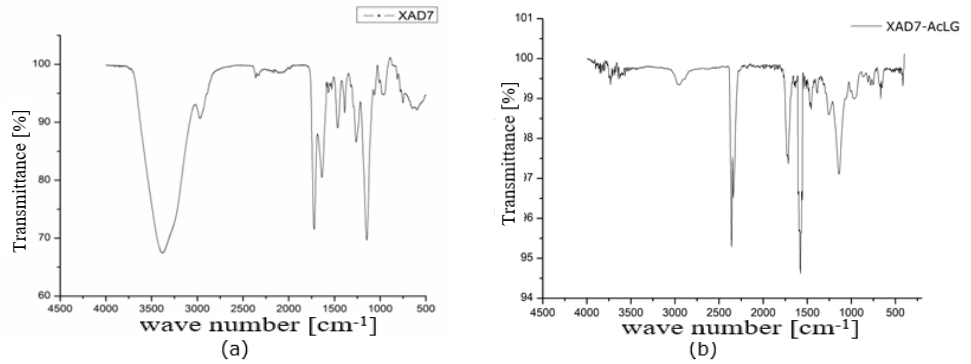

Figure 5.4. Recorded FT-IR spectrum for XAD7(a) and for the material XAD7-AcLG(b) [297] XAD7-AcLG(b) [297]

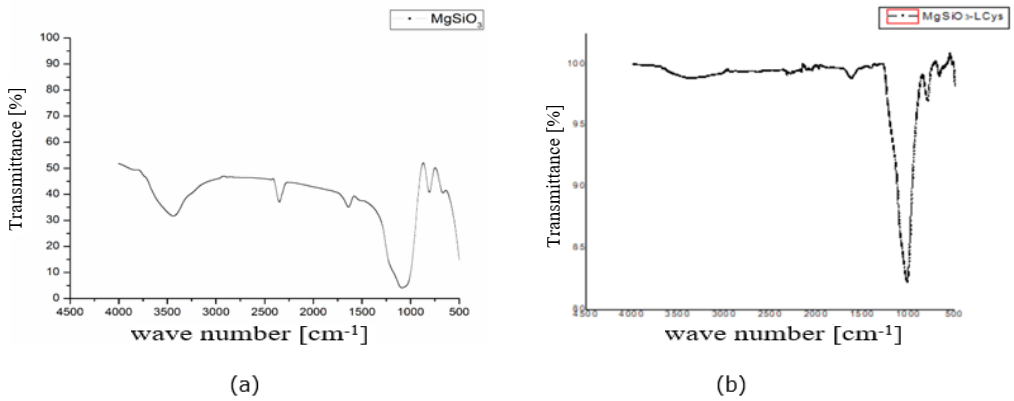

Figure 5.5. Recorded FT-IR spectrum for the support $MgSiO_3$(a) and the material $MgSiO_3$-LCys(b) [303]

From the FT-IR spectrum recorded for the support material Amberlite-XAD7, represented in Figure 5.4.a), it can be seen that around the wave number of 3440cm^{-1}, an absorption band specific to the stretching vibration of the group -OH appears, then at the wave numbers 2969 cm^{-1}, 2890 cm^{-1}, 1469 cm^{-1} and 1389 cm^{-1}, vibrations specific to the grouping -CH aliphatic occur, and at the wave numbers 1732 cm^{-1}, 1263 cm^{-1} with shoulders at 1294 cm^{-1} and 1317 cm^{-1} and at 1151 cm^{-1} there appear vibrations specific to the connection =CO, all these vibrations being specific to the Amberlite XAD7 resin [297, 304, 305]. From the FT-IR spectrum represented in Figure 5.4.b), recorded for XAD7-AcLG material at the wave number 3540 cm^{-1}, vibrations specific to the grouping -NH are observed. Around the wave number 3000 cm^{-1} there appear vibrations specific to the group –OH, and in the range of 1641-1353 cm^{-1} there appear vibrations specific to the bond =CO from the -COOH group or asymmetric vibrations of the group =CO from -COOH, specific to the amino acid L-glutamic [209, 297].

From the FT-IR spectrum represented in Figure 5.5.a) for $MgSiO_3$ it can be seen that around the wave number 1032 cm^{-1}, an absorption band specific to the stretching vibration of the O-Si-O group appears [307]. From the FT-IR spectrum represented in Figure 5.5.b) for the $MgSiO_3$-LCys material it can be seen that around the wave number 1395 cm^{-1} there are vibrations specific to the C=O link from the -COOH group, at the wave number 1380 cm^{-1} there are vibrations specific to the Aliphatic C-H group, at the wave number 2550 cm^{-1}, specific vibrations of the S-H group appear, and at the wave number 1600 cm^{-1} there are observed vibrations specific to the N-H group that highlight the functionalization of the $MgSiO_3$ support with L-cysteine-specific groups.

Experimental data on the specific surface area and pore volume are presented in Table 5.5.

Table 5.5. Surface area and total pore volume for XAD7, XAD7-AcLG, $MgSiO_3$ and $MgSiO_3$-LCys

Material	Surface, [m^2/g]	Total pore volume, [cm^3/g]
XAD7	300.00	0.44
XAD7-AcLG	275.00	0.48
$MgSiO_3$	289.00	0.33
$MgSiO_3$-LCys	166.00	0.43

The total pore volume for XAD7-AcLG and $MgSiO_3$-LCys materials increases following the functionalization of the supports, which confirms that the extractants penetrate inside the pore of the supports.

Atomic force microscopy, AFM:

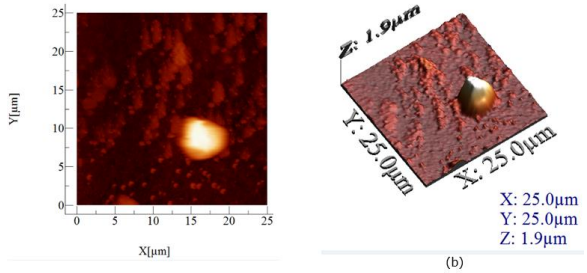

Figure 5.8. 2D(a) and 3D(b) views for XAD7-AcLG material on a surface (25 µm x 25 µm); Z = 1,9 µm in the 3D representation [310]

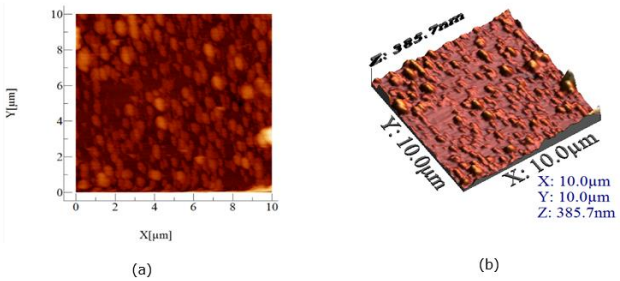

Figure 5.11. 2D(a) and 3D(b) views of $MgSiO_3$-LCys material on a surface (10 µm x 10 µm); Z = 0.3857 µm in the 3D representation

AFM is one of the most used techniques of scanning probe microscopy (SPM- Scanning Probe Microscopy) and has been used for the topographical analysis of the surfaces of materials obtained by functionalization XAD7-AcLG and $MgSiO_3$-LCys, thus highlighting the morphological changes due to the chemical functionalization of these new materials.

Determination of zero load potential, pH_{pZc}:

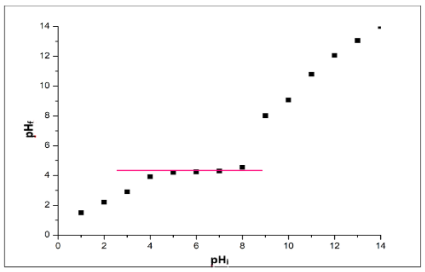

Fig.5.20

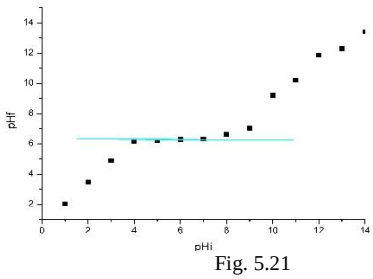

Fig. 5.21

pH_{final} dependence on $pH_{initial}$ for XAD7-AcLG material (Figure 5.20) and $MgSiO_3$-LCys material (Figure 5.21)

Knowing of the acid-base properties of adsorbent material XAD7-AcLG and $MgSiO_3$-LCys it could be generate information on their use. Based on the determination of the pH_{pZc} it was established that the XAD7-AcLG material has pH_{pZc}~4, and the $MgSiO_3$-LCys material has pH_{pZc}~6,2; cation adsorption is favored at pH values > pHpzc and adsorption of anions is favored at pH values < pH_{pzc}.

CHAPTERS 6 AND 7. APPLICATIONS OF XAD7-AcLG MATERIAL FOR THE ADSORPTION RECOVERY OF Au(III) AND $MgSiO_3$-LCys MATERIAL FOR THE RECOVERY OF Pd(II) FROM WASTE SOLUTIONS

Recovery of Au(III) and Pd(II) from waste solutions by static adsorption

In static mode, in order to establish the conditions under which the gold and palladium ions can be recovered from the used solutions, by adsorption, the role of the process-specific parameters was studied, namely: the ratio S : L, the pH of the solution containing the metal ions, the contact time, the temperature and the initial concentration of the solutions containing Au(III) and Pd(II).

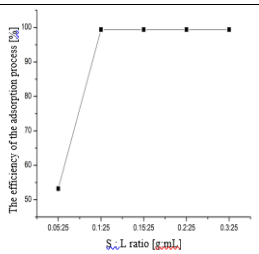	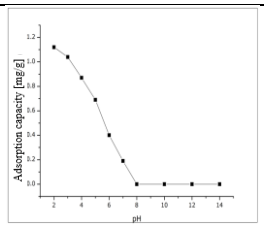	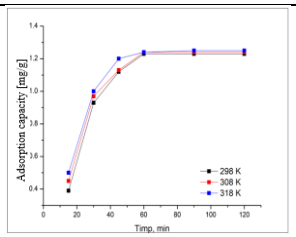	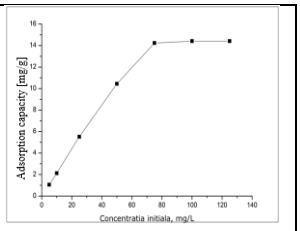
Dependence of the efficiency of the adsorption process of Au (III) on the ratio S : L	The effect of the pH of Au (III) solutions on the adsorption capacity of the material XAD7-AcLG	Influence of contact time and temperature on the adsorption capacity of XAD7-AcLG material	Influence of the initial concentration of Au (III) solution on the adsorption capacity of XAD7-AcLG material

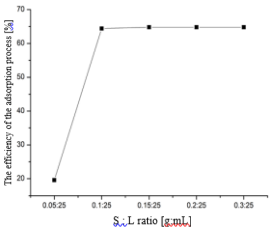

Dependence of the efficiency of the Pd (II) adsorption process on the S: L ratio

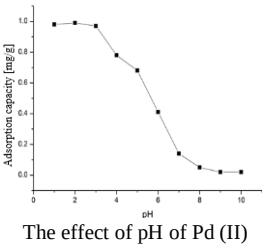

The effect of pH of Pd (II) solutions on the adsorption capacity of $MgSiO_3$-LCys material

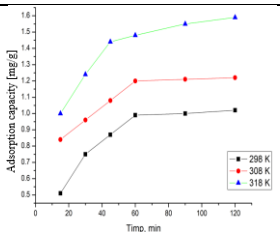

Influence of contact time and temperature on the adsorption capacity of $MgSiO_3$-LCys material

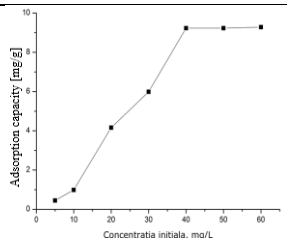

Influence of the initial concentration of Pd (II) solution on the adsorption capacity of $MgSiO_3$-LCys material

The following were found:

- the maximum efficiency of the adsorption process of Au and Pd ions is at the ratio S : L = 0,1g : 25 mL;
- the contact time affects the adsorption process and has been set to be 60 min;
- the adsorption of Au ions proceeds with a good adsorption capacity at pH < 4 and Pd ions at pH<3;
- the maximum adsorption capacity of the XAD7-AcLG material is 14.23 mg Au(III)/g, for an initial au(III) concentration of ~75 mg Au(III)/L;
- and mgSiO3-LCys material is 9.23 mg Pd(II)/g for an initial concentration of Pd(II) of ~40 mg Pd(II)/L.

In order to describe the adsorption mechanism of Au(III) and Pd(II) on the two materials, XAD7-AcLG and $MgSiO_3$-LCys, respectively, kinetic, thermodynamic and equilibrium studies have been carried out. The influence of the contact time, temperature, initial concentration of metal ions on the adsorption capacity, the activation energy value was monitored and the model of the mechanism that describes with the best accuracy the adsorption process studied was established.

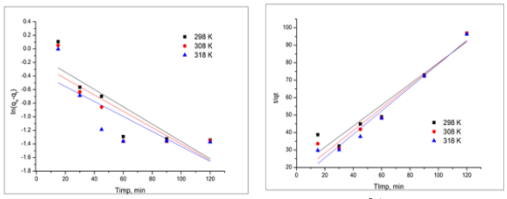

a) b)

Figure 6.6. The pseudo-order-one(a) kinetic pattern, and pseudo-order-two (b) for the recovery process of Au(III) by adsorption on XAD7-AcLG material

Temperature [K]	The pseudo-order-one kinetic pattern				The pseudo-order-two kinetic pattern			
	$q_{exp.}$ [mg/g]	k_1 [min^{-1}]	$q_{calc.}$ [mg/g]	R^2	$q_{exp.}$ [mg/g]	k_2 [g/mg·min]	$q_{calc.}$ [mg/g]	R^2
298	14,2300	0,0047	5,4500	0,7626	14,2300	36,7400	11,8200	0,9309
308	14,2400	0,0061	5,2400	0,7125	14,2400	41,9300	12,2500	0,9561
318	14,2500	0,0069	5,2500	0,6372	14,2500	47,4600	12,2500	0,9680

Table 6.5. Kinetic data obtained in the recovery process of Au(III) by adsorption on XAD7-AcLG material

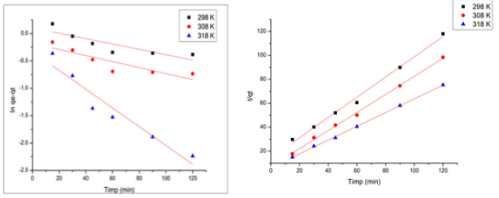

a) b)

Fig. 7.6. The pseudo-order-one(a) kinetic pattern, and pseudo-order-two (b) for the recovery process of Pd(II) by adsorption on $MgSiO_3$-LCys material

Temperatura (K)	The pseudo-order-one kinetic pattern				The pseudo-order-two kinetic pattern			
	$q_{exp.}$ [mg/g]	k_1 [min^{-1}]	$q_{calc.}$ [mg/g]	R^2	$q_{exp.}$ [mg/g]	k_2 [g/mg min]	$q_{calc.}$ [mg/g]	R^2
298	0.99	0.0049	1.18	0.7526	0.99	0.0974	1.11	0.9941
308	1.21	0.0055	1.32	0.7198	1.21	0.2515	1.19	0.9979
318	1.55	0.0171	1.74	0.9270	1.55	0.4894	1.40	0.9994

Tabel 7.5. The kinetic data which are obtained in the recovery process of Pd(II) by adsorption on $MgSiO_3$-LCys material

From the kinetic studies it has been found that the order-two pseudo kinetic model is one of the best models for the experimental data; this is apparent from the values of the coefficient of determination R^2, which is close to the value 1 both in the case of retension Au(III) and in the case of retention of Pd(II).

Based on the experimental data, the activation energy was calculated, it is 10.07 KJ/mol

for the recovery process by adsorption of Au ions on the XAD7-AcLG material and 15.6 KJ/mol for the adsorption recovery process of Pd ions on $MgSiO_3$-LCys material. These values being higher than 8 kJ/mol, it is considered that the adsorption process is of a physico-chemical nature.

ΔH^0, [kJ/mol]	ΔS^0, [J/mol·K]	ΔG^0, [kJ/mol]			R^2
		298 K	308 K	318 K	
15.43	55.8	-1.22	-1.77	-2.33	0.9718

a) – Table 6.6

ΔH^0, [kJ/mol]	ΔS^0, [J/mol·K]	ΔG^0, [kJ/mol]			R^2
		298 K	308 K	318 K	
15.4	81.06	-8.72	-9.53	-10.34	0.9963

b) – Table 7.6

Thermodynamic parameters for the Au(III) adsorption recovery process on XAD7-AcLG material (a – Table 6.6) and a Pd(II) on $MgSiO_3$-LCys (b – Table 7.6)

Thermodynamic parameters were determined from the slope of the line and value at origin of the linear representation of ln K_d = f(1/T); thus, it was established that the processes of recovery of gold and palladium ions by adsorption are:
- endothermic processes -> because the values of variation of the free enthalpy ΔH° are positive;
- are spontaneous processes -> because the values of the free energy variation Gibbs ΔG° , calculated from the experimental data, are negative and in absolute value increase with the temperature;
- are processes of physico-chemical nature, taking place at the solid-liquid interface - > given the positive values of the free entropy variation ΔS°.

The mechanism of the Au(III) adsorption process on XAD7-AcLG material and Pd(II) on $MgSiO_3$-LCys material was established using Langmuir, Freundlich and Sips models. The parameters specific to each isothermal used to model the experimental data are obtained from the slope of the straight and ordered at the origin.

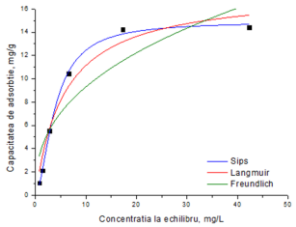

Fig. 6.9. Adsorption isothermals for the absortion process of Au(III) on XAD7-AcLG material

$q_{exp.}$ [mg/g]		14.2300
The isotherms	Adsorption isotherm parameters	
Langmuir	q_0 [mg/g]	17.6000
	K_L [L/mg]	0.1700
	R^2	0.9557
Freundlich	K_F [mg/g]	3.7600
	$1/n_F$	0.3900
	R^2	0.8004
Sips	q_0 [mg/g]	14.9000
	K_s	0.3200
	$1/n_s$	0.7100
	R^2	0.9972

Table 6.7. Parameters of the adsorption isothermals for the recovery absorption process of **Au(III)** on the material XAD7-AcLG

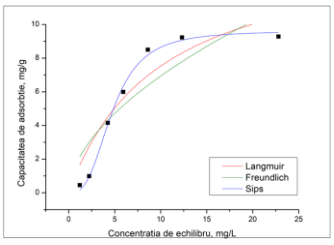

Fig. 7.9. Adsorption isothermals for the absortion recovery process of Pd(II) on the material XAD7-AcLG

q_{exp} (mg/g)		9.23
The isotherms	Parameters	
Langmuir	q_0 [mg/g]	14.9500
	K_L [L/mg]	0.1010
	R^2	0.8688
Freundlich	K_F [mg/g]	1.9300
	$1/n_F$	0.5500
	R^2	0.7599
Sips	q_0 [mg/g]	9.6700
	K_s	$7.03 \cdot 10^{-2}$
	$1/n_s$	2.2000
	R^2	0.9902

Table 7.7. Parameters of the adsorption isothermals for the absorption recovery process of Pd(II) on the material $MgSiO_3$-LCys

It has been found that it is the Sips isothermal that best shapes the experimental data obtained, since the coefficient of determination R^2 is ~ 1 both for Au(III) and in the case of adsorption retention of Pd(II).

Recovery of Au(III) and Pd(II) from waste solutions by dynamic adsorption

In dynamic mode, studies have been carried out on the recovery of Au(III) and Pd(II) from the waste solutions by the adsorption process in the fixed-bed adsorption column, a process shown schematically in Figure 6.10.

Important parameters for evaluating the efficiency of the adsorbent material used in dynamic regime are: effluent flow in the column, height of the fixed layer and time.

In order to determine the adsorption mechanism of Au(III) and Pd(II) and to design the adsorption process in dynamic mode, it is necessary to know the evolution of the residual concentration of the effluent at a given time.

The performances of the adsorption process in the fixed bed adsorption column are evidenced by the study of the penetration curves, i.e. by the evolution of the residual concentration of metal ions in relation to their initial concentration (C_{rez}/C_0) as a function of the effluent volume passed through the column, for distinct quantities of adsorbent material.

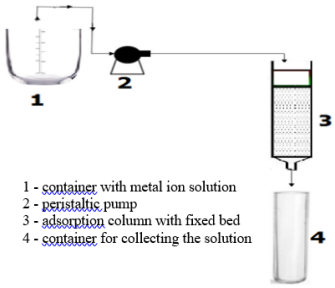

Fig. 6.10 The scheme of the adsorption process in dynamic regime, in column with fixed bed

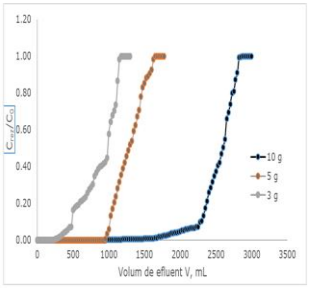

Fig. 6.11 Graphical representation of penetration curves for adsorption of Au(III) on XAD7-AcLG function of effluent volume

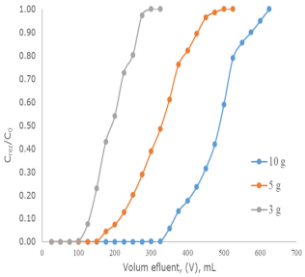

Fig. 7.10 Graphical representation of penetration curves for Pd(II) adsorption on $MgSiO_3$-LCys $MgSiO_3$-LCys depending on the effluent volume

The obtained experimental data are used at correlating the volume of effluent passed over the quantities, respectively, different heights of adsorbent materials, with the time it takes to pierce the adsorption columns. These data were modeled with three mathematical models, namely, the Bohart-Adams model, the Yoon-Nelson model and the Thomas model.

The amount of material, $m_{adsorbent}$ [g]	The empirical model			Saturation concentration, N_0, [mg/L]	Theoretical time, τ, [min]	Theoretical adsorption capacity, q_{th}, [mg/g]]
	K_{B-A} [l /mg·min]	K_{Y-N} [1/min]	K_{Th} [l/mg·min]			
10	$8.6 \cdot 10^{-4}$	$6.3 \cdot 10^{-2}$	$1.02 \cdot 10^{-3}$	1099.6	320.23	13.37
5	$7.5 \cdot 10^{-4}$	$5.7 \cdot 10^{-2}$	$1.05 \cdot 10^{-3}$	1141.9	159.20	13.37
3	$7.4 \cdot 10^{-4}$	$2.5 \cdot 10^{-2}$	$1.56 \cdot 10^{-3}$	1146.2	97.09	13.52
Regression coefficient, R^2				Experimental time, [min]		Experimental adsorption capacity, [mg/g]
10	0.9644	0.9806	0.9836	281.25		12.53
5	0.9747	0.9854	0.9869	118.75		11.35
3	0.9803	0.9883	0.99 47	87.50		11.07

Table 6.9. Parameters of the **A(III)** adsorption recovery process dynamic mode in fixed bed adsorption column

The amount of material, $m_{adsorbent}$ [g]	The empirical model			Saturation concentration, N_0, [mg/L]	Theoretical time, τ, [min]	Theoretical adsorption capacity, q_{th}, [mg/g]
	K_{B-A} [L/mg·min]	K_{Y-N} [1/min]	K_{Th} [L/mg·min]			
10	$3.45 \cdot 10^{-5}$	0.2137	$2.50 \cdot 10^{-5}$	1688.8	24.40	3.33
5	$1.89 \cdot 10^{-5}$	0.1376	$2.29 \cdot 10^{-5}$	1960.8	46.05	3.88
3	$1.90 \cdot 10^{-5}$	0.1469	$2.99 \cdot 10^{-5}$	1407.7	68.30	2.85
Regression coefficient, R^2				Experimental time, [min]		Experimental adsorption capacity, [mg/g]
10	0.9717	0.9722	0.9704	89.285		1.97
5	0.9777	0.9941	0.9961	78.571		0.86
3	0.9755	0.9727	0.9911	57.142		0.19

Table 7.9. Parameters of the adsorption process **Pd(II)** recovery in dynamic mode, in fixed bed adsorption column

From the data base of the parameters of the recovery processes of Au(III) and Pd(II) in dynamic mode in fixed bed adsorption column, it is noted that all three applied models described the adsorption of Au(III) on the XAD7-AcLG material in a good way and, respectively, of Pd(II) on $MgSiO_3$-LCys, depending on the variation in the amount of adsorbent material, respectively, by the variation in the height of the adsorbent layer.

For all mathematical models used, the coefficient of determination R^2 has values close to the value 1, which demonstrates the validity of the data obtained from mathematical modelling.

For the recovery of Au(III) and Pd(II), in the case of the Thomas model, from the obtained results, it can be found that with the increase in the height of the material layer in the adsorption column, the Thomas constant, $k_{Th,}$ decreases. The reason associated with this decrease is represented by the motor force necessary for the adsorption process, given by the difference between the concentration of the adsorbed metal on the material and the concentration of the metal ions in the solution. It is also noted that the determination coefficient R^2 decreases. The adsorption capacity of the adsorbent established materials from the model is approximately the same as the value of the experimentally established adsorption capacity, both for the adsorbed gold ions and for the palladium ions. It can therefore be assumed that this model describes in the best way the mechanism of the adsorption process of Au(III) and Pd(II) in dynamic mode, on the fixed bed adsorption column.

The profitability, feasibility and sustainability of an adsorption process are influenced by the regeneration possibilities of the adsorbent material. Desorption studies shall prove the practical applicability of the adsorption process regarding the reuse of the fixed layer of adsorbent material in the column after exhaustion. In the study on the desorption process of Au(III) from XAD7-AcLG material and Pd(II) from $MgSiO_3$-LCys, it was used as a desorption agent HNO_3 5%, for XAD7-AcLG material in 5 adsorption-desorption cycles (with a desorption degree between 83% - 34%) and for $MgSiO_3$-LCys material in 3 adsorption-desorption cycles (with a desorption degree between 52.5% - 12.9%).

The XAD7-AcLG and $MgSiO_3$-Lcys materials depleted following Au(III) and Pd(II) recovery were calcined to obtain gold and metallic palladium respectively. Calcining was performed at a temperature of 600^0C, for 240 min, with an oven heating rate of 5^0C/min. To highlight the obtaining of metallic gold and metallic palladium, the samples obtained after calcination were characterized by scanning electron microscopy and X-ray spectroscopy by energy dispersion.

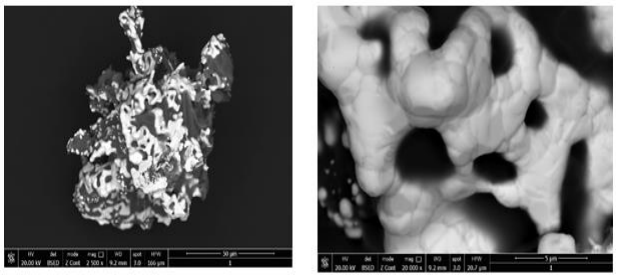

Figure 6.19. SEM views obtained from the calcination of the exhausted XAD7-AcLG material for Au recovery [297]

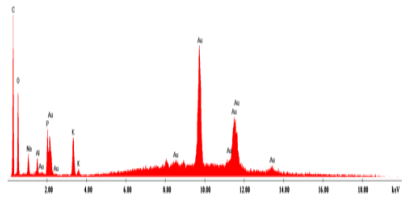

Element	C	O	Na	Si	P	K	Au	Total
Wt, [%]	23,18	39,20	8,59	1,10	9,02	9,19	9,72	100,00

Figure 6.20. EDX obtained from the calcination of the exhausted XAD7-AcLG material in order to recover the metallic gold [297]

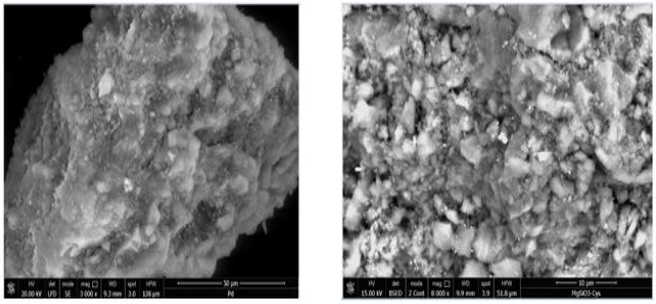

Figure 7.16. SEM images obtained after the calcination of the exhausted $MgSiO_3$-LCys material, in order to recover the palladium

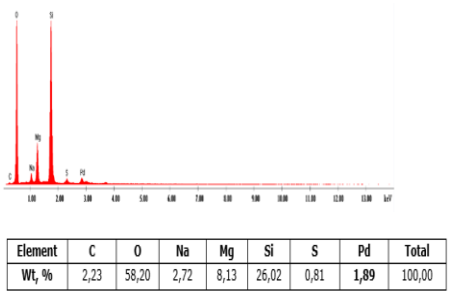

Element	C	O	Na	Mg	Si	S	Pd	Total
Wt, %	2,23	58,20	2,72	8,13	26,02	0,81	1,89	100,00

Figure 7.17. EDX obtained by calcining the exhausted $MgSiO_3$-LCys material, in order to recover the palladium

A process of recovery of metallic gold, coming from waste solutions, by adsorption on the XAD7-AcLG material, followed by its calcination after exhaustion, is presented

schematically in Figure 6.21. The obtained metallic gold can be subsequently reintroduced into specific technological processes.

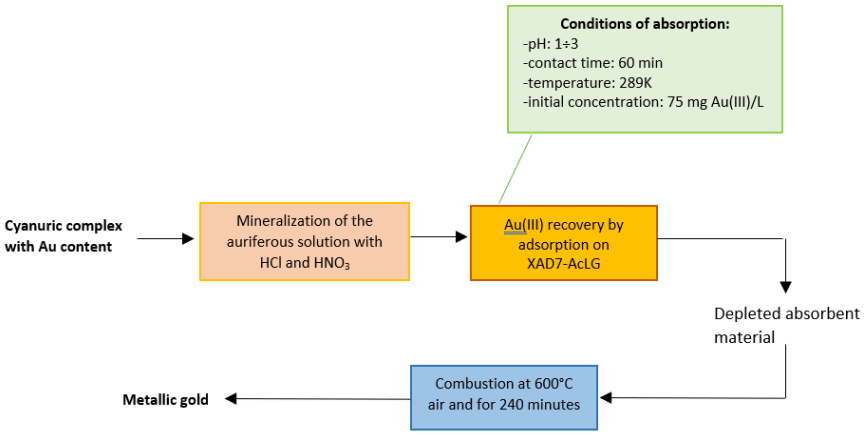

Figure 6.21. Process of recovering metallic gold from used solutions [297]

A process of recovery by adsorption of metallic palladium from $MgSiO_3$-LCys material, followed by its calcination after exhaustion, is shown schematically in Figure 7.18. Metal palladium mixed with magnesium silicate can be reintroduced into specific technological processes.

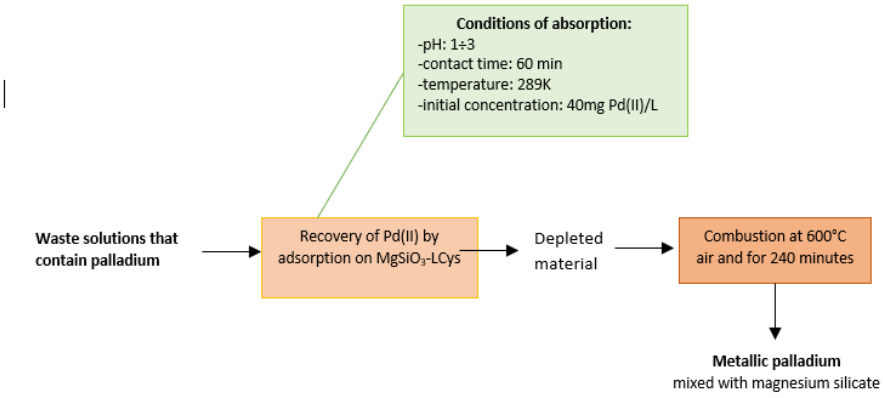

Figure 7.18. Recovery process of metal palladium from worn solutions

CHAPTER 8. OPTIMIZATION OF THE Au(III) AND Pd(II) ADSORPTION PROCESS BY FACTORIAL DESIGN

In the framework of a factorial experiment, the aim is to identify the factors that lead to the best possible adsorption capacity; the experimental data were centralised in the form of matrices and processed to characterise the poces.

Optimization of the adsorption process determines the setting range of the influential input factors that provide the best response to the process. There were also used nonlinear experiments (response surface design, RSD), aiming that the process response to target the output variable, identifying the range of values of the input factors with which a maximum value can be obtained.

Objective functions (dependent variables) define and quantitatively evaluate the behavior and evolution trends of the system under investigation, under normal conditions.

The effects and interactions of processes were tracked by optimizing different parameters: pH, temperature, contact time, initial concentration. They were tracked in order to obtain a maximum adsorption capacity of the XAD7-AcLG material.

A schematic presentation of the adsorption pattern studied is represented below:

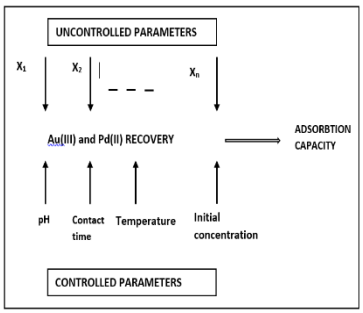

Model of the adsorption process of Au(III) si Pd(II)

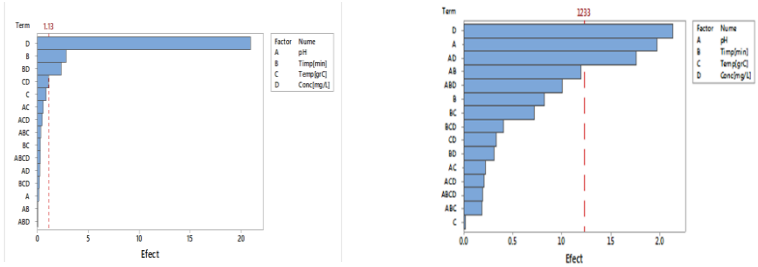

Pareto diagram - the effect of control parameters on the adsorption capacity of XAD7-AcLG (a) și $MgSiO_3$-LCys (b) materials

The factorial experiment consisted of a series of complete tests in which all possible combinations of the levels of setting the control factors followed, in this case, of the parameters that significantly influence the adsorption capacity were performed, namely: pH, temperature, contact time and initial concentration. They were tracked for the purpose of obtaining a maximum adsorption capacity of the new adoring materials, XAD7-AcLG and $MgSiO_3$-Lcys. The experiments aimed at optimizing the adsorption process were carried out in two stages, namely:

- in the first stage, the aim was to determine the variables that have an important significance on the adsorption process and to determine the controllable factors in order to obtain a maximum of the adsorption capacity; 16 runs were performed each in the case of Au(III) retention in case of retention of Pd(II). It was found that on the adsorption process studied, in fact on the adsorption capacity of XAD7-AcLG material have a significant effect (i) the contact time and (ii) the initial concentration of the solution containing **Au(III)**; in the case of $MgSiO_3$-LCys material, three factors have been found to have a significant effect on the adsorption process, namely: pH, contact time and initial concentration of the solution containing **Pd(II)**;

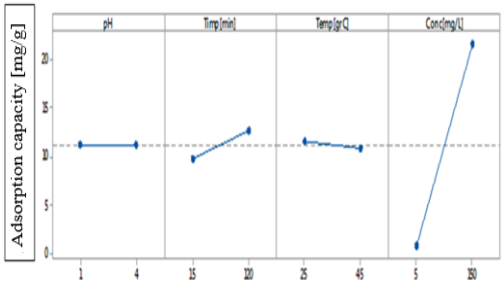

Fig. 8.3. Main effects of control factors on the adsorption capacity of XAD7-AcLG material

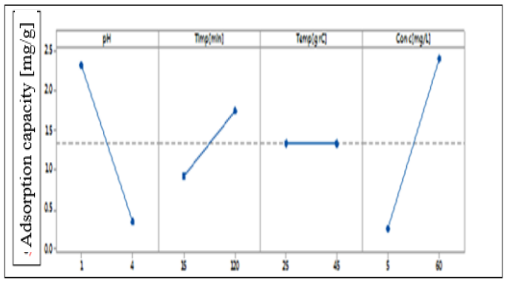

Figure 8.18. Main effects of control factors on the adsorption capacity of $MgSiO_3$-LCys material

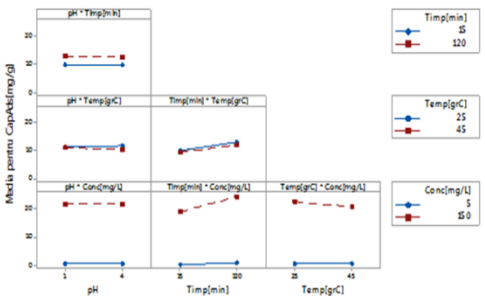

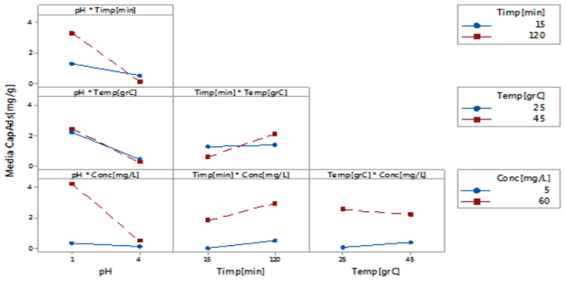

Figure 8.4. Interactions between control factors and the response of the adsorption process (adsorption capacity) of Au(III) ions on XAD7-AcLG material [310]

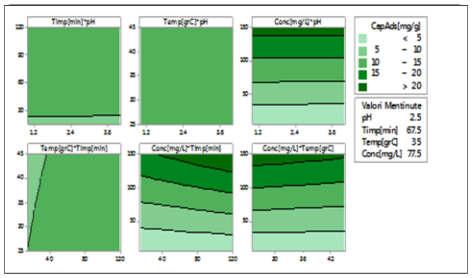

Figure 8.5. 2D contour curves for pH, contact time, temperature and initial concentration if the response is adsorption capacity, for XAD7-AcLG material [310]

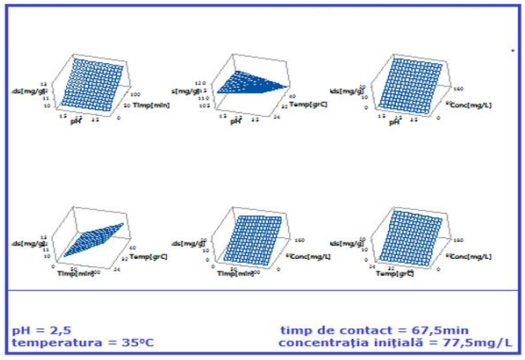

Figure 8.6. 3D contour curves for pH, contact time, temperature and initial concentration where the response is the adsorption capacity for the XAD7-AcLG material [310]

Figure 8.18. Interactions between control factors and the response of the adsorption process (adsorption capacity) of Pd(II) ions on $MgSiO_3$-LCys material

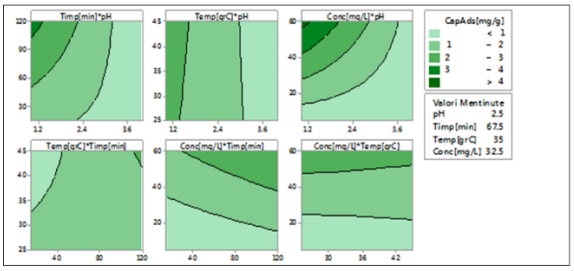

Figure 8.19. 2D contour curves for pH, contact time, temperature and initial concentration where the response is the adsorption capacity for $MgSiO_3$-LCys material

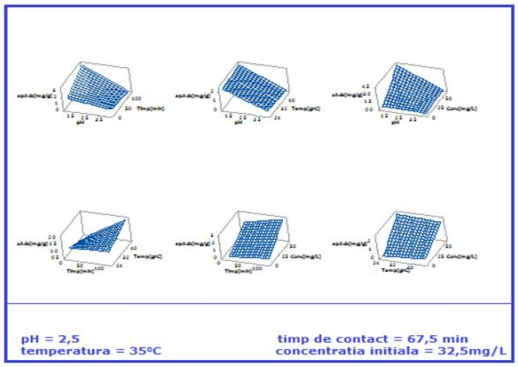

Figure 8.20. 3D contour curves for pH, contact time, temperature and initial concentration where the response is the adsorption capacity for $MgSiO_3$-LCys material

- in the 2nd stage, the response surface (RSD) models were designed. There were 12 runs in the case of Au(III) detention and 19 runs in the case of Pd(II) detention.

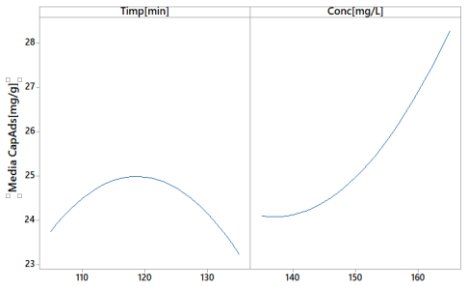

Figure 8.10. Main effects of controlled factors (contact time and initial concentration) on the adsorption capacity of Au(III) on the XAD7-AcLG material

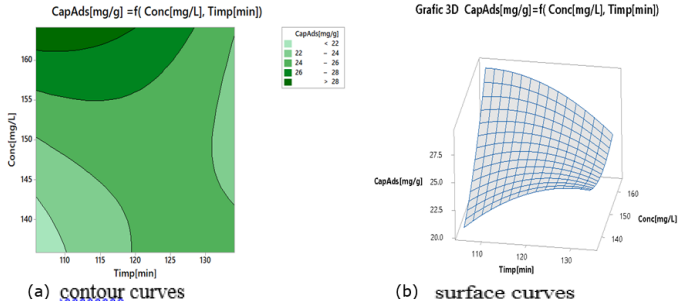

Figure 8.12. Contour curves (a) and surface curves (b) for the initial contact time and concentration if the response is the adsorption capacity of Au(III) on the XAD7-AcLG material [310]

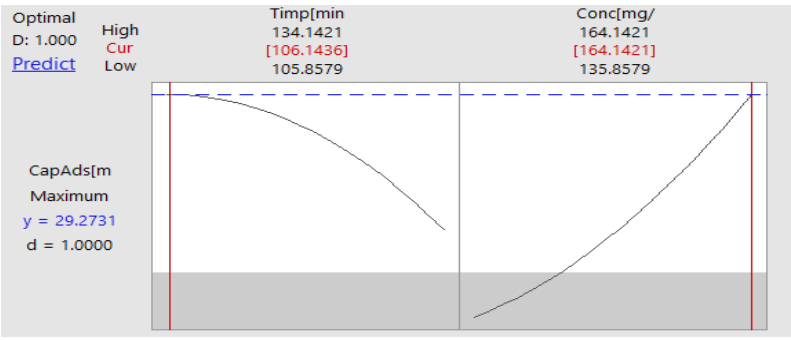

Figure 8.13. Step II, optimizing the response of the Au(III) adsorption process on XAD7-AcLG material [310]

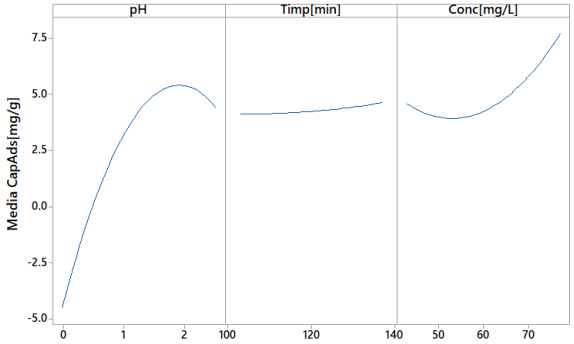

Figure 8.24. Main effects of controlled factors on the adsorption capacity of $MgSiO_3$-LCys material

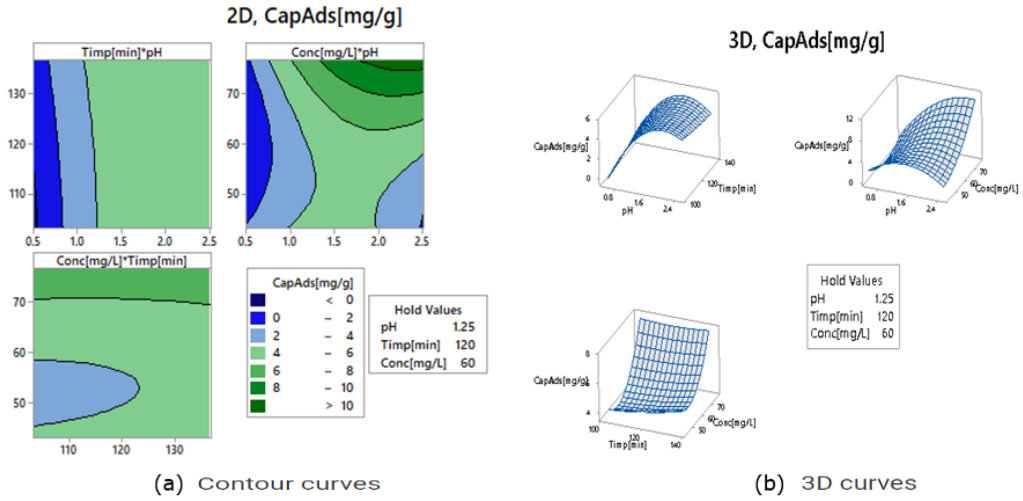

Figure 8.26. Contour curves (a) and 3D (b) curves for pH, contact time and initial concentration if the answer is the adsorption capacity of $MgSiO_3$-LCys material

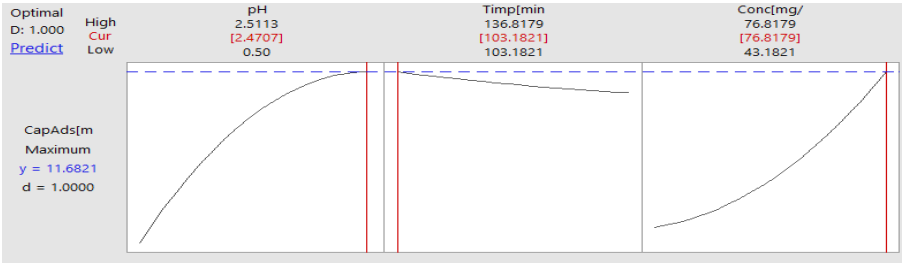

Fig.8.27. Optimisation of the response of the Adsorption process of Pd(II) on $MgSiO_3$-LCys material

CHAPTER 9. FINAL CONCLUSIONS. ORIGINAL CONTRIBUTIONS

In **the first Part of the doctoral thesis,** it is presented the literature study that refers to the identification of the current state of the research in the proposed topic.

In **Part II of the doctoral thesis** are presented the original contributions.

The research reflected in this doctoral thesis had as **main objective** the obtaining of new materials with properties designed for the recovery of Au(III) and Pd(II), given that these metals are known for their multiple applications and for their value.

In the undertaken studies, 80 materials were obtained by functionalization by impregnation, by SIR (Solvent Impregnated Solvent) method and by ultrasonication. As support were used two commercial resins of the type Amberlite XAD4 (styrene matrix-divinl-benzene) and Amberlite XAD7 (acrylic matrix), an inorganic support - magnesium silicate, $MgSiO_3$ and a biopolymer - cellulose, and as extractants were used the amino acids: L-glutamic acid (AcLG) and L-cysteine (LCys). The support ratio was varied: extractant, and in order to establish the optimal ratio, adsorption studies of Au(III) and Pd(II) were performed. It was aimed at establishing the most efficient method of functionalization by impregnation and establishing the materials with the best affinity for Au(III), respectively for Pd(II).

Thus, **the optimal ratio support : extractant** to obtain the best adsorption capacity was **1 g of support : 0.1 g extractant**. Both, through the functionalization by impregnation by the SIR method and by the functionalization by ultrasonication, the behavior of the materials during the adsorption was similar, but the ultrasonication is a faster process (10 min) unlike the CRS method (24 h), the subsequent synthesises were achieved by ultrasonication. Au(III) has been found to exhibit better affinity for XAD7-AcLG material and Pd(II) to exhibit better affinity for $MgSiO_3$-LCys material. The XAD4-AcLG, XAD4-LCys, C-AcLG and C-LCys materials show insignificant affinity for the two metal ions.

In order to highlight the presence of active groups specific to the two amino acids on the surface of the supports, a series of physico-chemical investigations were performed.

The active groups (-NH_2, -SH, -COOH) of the AcLG and LCys extractors significantly improve the adsorption capacity of the new materials, XAD7-AcLG and $MgSiO_3$-LCys. The images obtained by **scanning electron microscopy**, **SEM** confirm the presence of extractants on the surface of materials and **the energy dispersion X-ray spectroscopy, EDX**, indicates qualitatively the presence of atom-specific picks from the active groups of amino acids. Bond-specific vibrations with active clusters have been confirmed using **Fourier transform infrared spectroscopy (FT-IR).**

The three-dimensional images of the surfaces of XAD7-AcLG and $MgSiO_3$-LCys materials obtained by impregnation functionalization, generated by **atomic force microscopy - AFM,** highlight the morphological changes due to functionalization.

The specific areas of the materials (BET) were determined before and after their modification by functionalization with active groupings. It was found that the specific surface area decreases from 300 m^2/g for XAD7 to 275 m^2/g for XAD7-AcLG and from 289 m^2/g for $MgSiO_3$ to 166 m^2/g for $MgSiO_3$-LCys, which confirms that the pores of the supporting materials are occupied by extractants.

For both materials, the total volume of pores increases from 0.44 cm^3/g for XAD7 to 0.48 cm^3/g for XAD7-AcLG and from 0.33 cm^3/g for $MgSiO_3$ to 0.43 cm^3/g for $MgSiO_3$-LCys, which confirms that the impregnation functionalization of the supports was achieved either by the penetration of the amino acid into its pores or by adsorption at its surface.

Based on the determination of the $\mathbf{pH_{pZc}}$ it was established that the XAD7-AcLG material has $pH_{pZc} \sim 4$, and the $MgSiO_3$-LCys material has $pH_{pZc} \sim 6,2$; cation adsorption is favored at values $pH > pH_{pzc}$ and adsorption of anions is favored at values $pH < pH_{pzc}$.

In order to establish the conditions under which Au(III) and Pd(II) can be recovered

from the used solutions by **static mode adsorption**, the role of the process-specific parameters was studied, namely: ratio S : L; the pH of the solution with Au(III), respectively with Pd(II); contact time; the initial temperature and concentration of Au(III) and Pd(II) respectively.

The results are presented, for the recovery of Au(III) and Pd(II) in static mode:

Adsorbtion recovery of gold and palladium PARAMETERS:				
STATIC MODE	Au(III)		Pd(II)	
	ratio solid : liquid = 0,1 g : 25 mL		ratio solid : liquid = 0,1 g : 25 mL	
	pH = 1 ÷ 4		pH = 1 ÷ 3	
	$t_{contact}$ = 10 min, ultrasonic mode		$t_{contact}$ = 10 min, ultrasonic mode	
	T = 298 K		T = 298 K	
	q_{max} = 14,23 mg Au(III)/g pentru c_i = 75 mg Au(III)/L		q_{max} = 9,23 mg Pd(II)/g pentru c_i = 40 mg Pd(II)/L	
	STUDIES:			
	KINETIC STUDIES			
	pseudo-order-two	E_a = 10,1 KJ/mol	pseudo-order-two	E_a = 15,6 KJ/mol
	TERMODYNAMIC STUDIES			
	spontaneous, endothermic, physico-chemical process		spontaneous, endothermic, physico-chemical process	
	EQUILIBRE STUDIES			
	Sips		Sips	

At the same time, in order to describe the mechanism of the adsorption process, kinetic, thermodynamic and equilibrium studies have been carried out. The value of the activation energy and the maximum adsorption capacity of the materials have been established.

In addition to static adosrbtion, **dynamic mode adsorption** in the fixed bed adsorption column has as advantages the fact that: (i) the system involves continuous adsorption, the adsorbent being continuously in contact with the adsorbite; (ii) it is a light and inexpensive technique; (iii) may be used on an industrial scale.

The results are presented centrally, for the recovery of Au(III) and Pd(II) in **dynamic mode**:

Adsorption recovery of gold and palladium Parameters:				
DINAMIC MODE	Au(III)		Pd(II)	
	c_i = 60 mg Au(III)/L	Q = 8 mL/min	c_i = 60 mg Pd(II)/L	Q = 7 mL/min
	h coloana adsorbție , [mm]	m XAD7-AcLG , [g]	h coloana adsorbție , [mm]	m HgSiO3-LCys , [g]
	100	10	70	10
	50	5	35	5
	30	3	21	3
	Adsorption-desorption			
	5 cycles		3 cycles	
	degree of desorption = 83 ÷ 34 %		degree of desorption = 52,5 ÷ 12,9 %	

The factorial experiment consisted of a series of tests in which all possible combinations of the levels of setting the control factors followed, in this case, of the parameters that significantly influence the adsorption capacity were carried out.

The results are presented centrally, for the factorial experiment:

- in step 1 – linear parameters:

FACTORIAL EXPERIMENT							
I. LINEAR EXPERIMENTS							
Au(III)				Pd(II)			
PARAMETERS:							
pH = 4	t = 120 min	T = 298K	c_i = 150 mg Au(III) / L	pH = 1	t = 120 min	T = 298K	c_i = 60 mg Pd(II) / L
q = 25,63 mg Au(III) / g				q = 6,75 mg Pd(II) / g			
Proposed parameters for the second stage – NELINIAR EXPERIMENTS (RSD)							
timp, initial concentration				pH, timp, initial concentration			

- in stage 2 – nonlinear experiments (RSD):

EXPERIMENT FACTORIAL				
THE SECOND STAGE. NONLINEAR EXPERIMENTS (RSD)				
Au(III)		Pd(II)		
PARAMETERS:				
t = 105 ÷ 140 min	c_i = 140 ÷ 165 mg Au(III) / L	pH = 0,5 ÷ 2	t = 110 ÷ 130 min	c_i = 50 ÷ 80 mg Pd (II) / L
OPTIMIZTION				
t = 106 min	c_i = 164 mg Au(III) / L	pH = 2,47	t = 103 min	c_i = 76,8 mg Pd (II) / L
q = 22,44 ÷ 28,95 mg Au(III) / g		q = 11,68 mg Pd(II) / g		

In the end, **a simple scheme of work** was proposed as a support for a possible design of adsorption processes, using new, selected materials.

Because of the complex mechanisms involved in the adsorption process, the estimation of the value of the possible adsorption capacity of metal ions on the adsorbent materials obtained by impregnation functionalization, is made by empirical design procedures that are based on the conditions of adsorption balance and on the fact that models are used that assume that the new adsorbent materials are homogeneous.

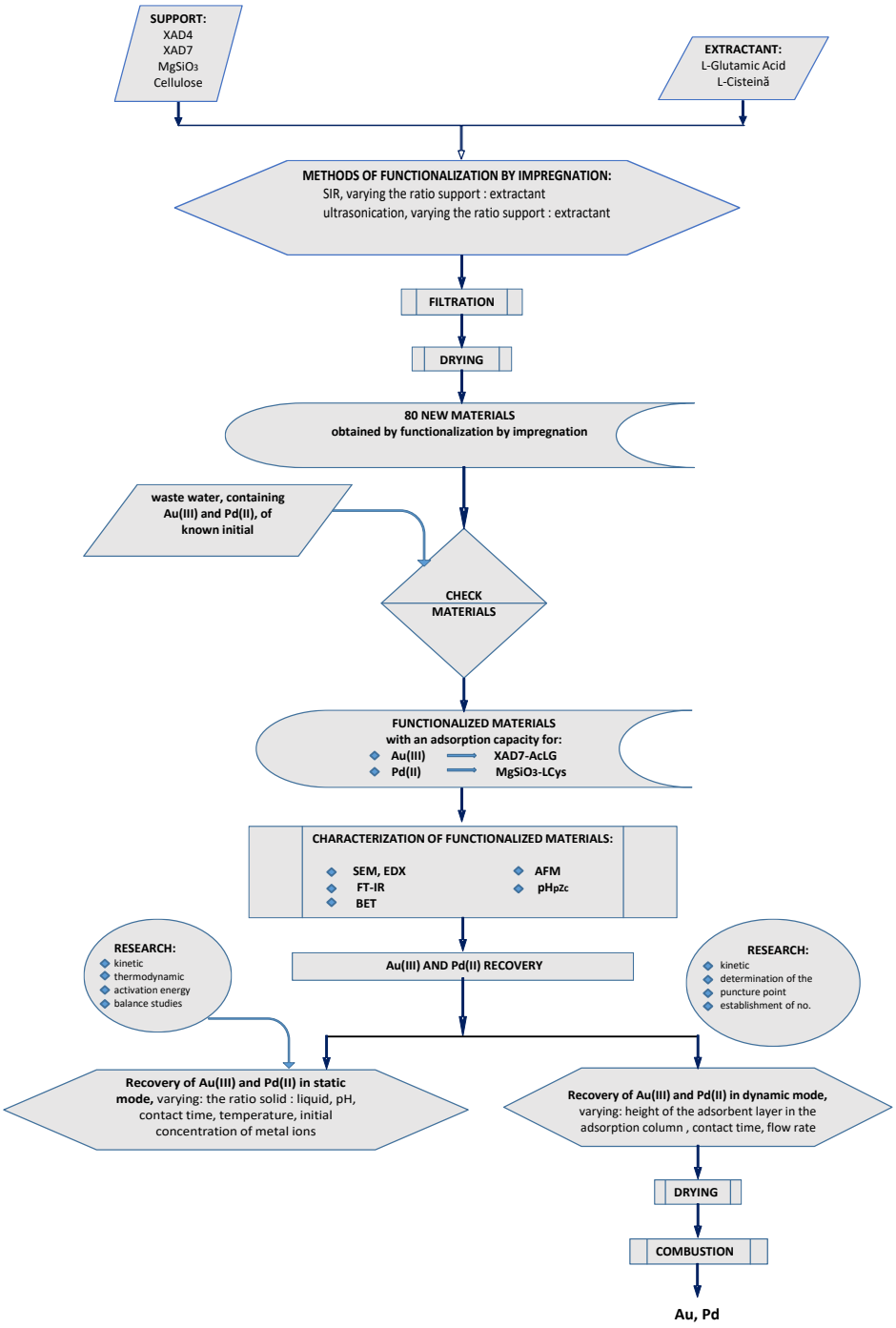

Figure 9.1. Scheme of work for the design of adsorption processes

The first part of the scheme presents the stages of obtaining the new adsorbent materials through impregnation functionalization and the scientific papers that were the basis for the selection of specific materials suitable for the retention of metal ions, namely, the obtaining of XAD7-AcLG material for the retention of Au(III) and $MgSiO_3$-Lcys material for the retention of Pd(II), as recorded in chapter 5 of the work and presented above.

The 2nd part of the scheme presents the physical-chemical investigations performed to highlight the presence of active groups specific to the two amino acids on the surface of solid supports. The materials selected for the studies, namely, XAD7-AcLG and $MgSiO_3$-LCys, were characterized by: SEM and EDX to confirm the presence of the active groups of extractants (namely the amiinic, thiolic and carboxylic groups), FT-IR for the identification of vibrations specific to the active groups of extractants, AFM to confirm the morphological changes due to

the functionalization by impregnation, BET for the determination of the specific surfaces that confirm the fact that the pores of the materials are occupied by extractors. The potential for pH_{pzc} zero load has also been determined, as recorded in chapter 5 of the paper and presented above.

The 3rd part of the scheme presents the stages of recovery of Au(III) and Pd(II) ions, in static and dynamic mode, including the establishment of the optimal parameters of these processes, as mentioned in chapters 6 and 7 of the work.

PERSPECTIVES

The perspectives of the research activity would be:

- deepening the studies on the application of the procedures for the recovery of Au(III) and Pd(II) from the waste solutions, developed within the doctoral thesis, for the recovery of other metals from wastewater, waters with complex chemical compositions, similar to those studied;

→ study of the use of Au(III) and Pd(II) extracted from waste water, for applications other than those strictly industrial.

In the work paper are mentioned 357 bibliographic references, here being presented a selection of them.

SELECTIVE BIBLIOGRAPHY

[61] M. Mihăilescu, P. Negrea, N. Dușeanu, A. Negrea, M. Ciopec, V. Gherman, R. Buzatu, M.Moțoc, "From the Complex Process of Gold Ions Recovery in New Antimicrobial Product", Revista de Chimie, București, 70(3), p. 1080, 2019

[122] R. Ruhela, A. K. Singh, B. S. Tomar, R. C. Hubli, "Separation of palladium from high level liquid waste – A review", Royal Sosiety of Chemistry, 4, p. 24344–24350, 2014

[139] A. Negrea, S. Ronka, M. Ciopec, N. Dușeanu, P. Negrea, **M.Mihăilescu**, "Kinetics, thermodynamics and equilibrium studies for gold recovery from diluted waste solution", Materials, 2021

[140] S. Syed, "Recovery of gold from secondary sources—A review", Hydrometallurgy 115-116 , p. 30–51, 2012

[205] F.L. Koon, M.F. Chi, L.Y. King, M. Gordon, "Selective adsorption of gold from complex mixtures using mesoporous adsorbents", Chemical Engineering Journal, 145, p. 185–195, 2008

[213] A. Dabrowski, "Adsorption - from theory to practice", Advances in Colloid and Interface Science, 93, p. 135-224, 2001

[216] K. Vasanth Kumar, K. Subanandam, V. Ramamurthi and S. Sivanesan, „GAC – problems and solutions", Green pages, Attleboro, MA 02703, SUA, 2004

[217] Y. Artioli, "Adsorption", Ecological Processes, p. 60-65, 2008

[219] N. Ayawei, A. Ebelegi, D. Wankasi, "Modelling and interpretation of adsorption isotherms," Journal of Chemistry, p. 1–11, 2017

[224] M.A. Al-Ghouti and D.A. Da'ana, "Guidelines for the use and interpretation of adsorption isotherm models: A Review", Journal of Hazardous Materials, 393 (122383), p. 1-22, 2020

[240] H. Patel „Fixed-bed column adsorption study: A comprehensive review". Applied Water Science, 9, p. 45, 2019

[256] A. Gabor, C. Davidescu, A. Negrea, M. Ciopec, P. Negrea, „Use of magnesium silicate functionalized with thiourea for Sr(II) and Tl(I) removal from polluted water," în WIT Transactions on Ecology and Environment, Water Pollution XIII, 2016

[295] B. Bittmann, F. Haupert, Alois K. Schlarb, "Ultrasonic dispersion of inorganic nanoparticles in epoxy resin", Elsevier, 2009

[297] M. Mihăilescu, A. Negrea, M. Ciopec, C. M. Davidescu, P. Negrea, N. Duţeanu, G.

Rusu, “Gold (III) adsorption from dilute waste solutions onto Amberlite XAD7 resin modified with L-glutamic acid”, Scientific Reports, 2019
[303] C. Vancea, **M. Mihăilescu**, A. Negrea, G. Moșoarcă, M. Ciopec, N. Duțeanu, P. Negrea, V. Minzatu, „Batch and Fixed-Bed Column Studies on Palladium Recovery from Acidic Solution by Modified $MgSiO_3$”, International Journal of Environmental Research *and* Public Health, 17, 9500, 2020
[306] L. Pablo, S. Mika, “Gold recovery from artificiala seawater using synthetic materials and seaweed biomass to induce gold nanoparticles formation in batch and column experiments”, Marine Chemestry, 152, p. 11-19, 2013
[310] M. Mihăilescu, A. Negrea, M. Ciopec, P. Negrea, N. Duțeanu, I. Grozav, P. Svera, C. Vancea, C.S. Dumitriu, “Full factorial design for gold recovery from industrial solution”, MDPI, Toxics, 9, 111, 2021
[312] V. Bellitto, „Atomic Force Microscopy- Imaging, Measuring and manipulating surfaces at the atomic scale”, Ed.; Intechopen, p. 147-174, 2012
[324] K. V. Kumar, K. Subanandam, V. Ramamurthi, S. Sivanesan, „GAC absorption process: problems and solutions”, Green Pages, March 2004
[332] K.Y. Foo, B.H. Hameed, ”Insights into the modelling of adsorption isotherm systems”, International Journal of Computer Applications in Chemical Engineering, 156, pp. 2–10, 2010
[337] A. Negrea, **M. Mihăilescu**, G. Mosoarca, M. Ciopec, N. Duteanu, P. Negrea, V. Minzatu, „Estimation on Fixed-Bed Column Parameters of Breakthrough Behaviors for Gold Recovery by Adsorption onto Modified/Functionalized Amberlite XAD7”, International Journal of Environmental Research and Public Health, 17, 6868, 2020
[341] M.S. Shafeeyan, W. Daud, A. Shamiri, “A review of mathematical modeling of fixed-bed columns for carbon dioxide adsorption”, Chemical Engineering Research and Design, 92(5):961–988, 2014
[353] A. Gabor, C. Davidescu, A. Negrea, M. Ciopec, I. Grozav, P. Negrea și N. Duțeanu, „Optimizing the Lanthanum adsorption process onto chemically modified biomaterials using factorial and response surface design,” Journal of Environmental Management, vol. 204, p. 839-844, 2017